

## Polarization of Water in the First Hydration Shell of $K^+$ and $Ca^{2+}$ Ions

Denis Bucher and Serdar Kuyucak\*

*School of Physics, University of Sydney, NSW 2006, Australia*

*Received: May 28, 2008; Revised Manuscript Received: July 29, 2008*

Accurate representation of the interactions of water molecules with charges is essential for correct description of biomolecules and their interactions and, hence, is a primary concern in the design of classical force fields. This task is made even more challenging by the fact that the charge distribution of water molecules in liquid is significantly altered by the local environment. To understand how such polarization effects would modify the force fields, we have performed density functional calculations for ion–water clusters using  $K^+$  and  $Ca^{2+}$  ions as probes. We find that the dipole moment of water molecules in the first hydration shell decreases with increasing number of waters, which is explained by the suppression of the ion's electric field by those of water dipoles. Adding further water beyond the first shell, the dipole moment of the first shell waters increases because water dipoles are strongly polarized in the presence of hydrogen bond acceptors. Thus the net polarization of water in the hydration shell of an ion is determined by two competing effects, of which only one directly depends on the ion. These observations explain why the dipole moment of waters in the first hydration shell of a  $K^+$  ion is smaller compared to those in bulk water while the opposite is true for  $Ca^{2+}$  ions and suggest new constraints to be used in the development of polarizable water models.

### Introduction

Water is the largest component of living cells and plays an active role in every aspect cellular function.<sup>1</sup> Therefore, an impressive amount of research has been devoted to the description of water–water and water–solute interactions.<sup>2–4</sup> A complicating factor in this endeavor is the polarizable nature of water molecules, which makes modeling of ion–water interactions a challenging task. In nonpolarizable force fields, commonly used in molecular dynamics simulations, polarization effects are approximately taken into account by increasing the partial charges on atoms. For example, in the case of a water molecule, its dipole moment is boosted from 1.86 to 2.27 D in the SPC model<sup>5</sup> and to 2.35 D in the TIP3P model.<sup>6</sup> While such a mean field approximation works reasonably well in bulk situations, for which they are optimized, problems arise when dealing with inhomogeneous systems such as interfaces,<sup>7–9</sup> pores,<sup>10–12</sup> and cavities.<sup>13,14</sup> To deal with such systems, it is necessary to include the polarization interaction explicitly in the classical force fields. Although there have been substantial efforts in this direction, a general purpose polarizable force field for simulation of biomolecules is yet to be developed (see, e.g., the reviews,<sup>3,15</sup> and the special issue of *Journal of Chemical Theory and Computation*).<sup>16</sup>

The main difficulty in modeling of polarization at the classical level stems from the fact that polarizability of individual atoms in a molecule cannot be measured by experiments. This leads to considerable arbitrariness in the methods employed for the description of polarization and the way they are parametrized. An alternative strategy that has recently become feasible is to use results of ab initio calculations in constraining the form and parameters of polarizable models. Thanks to the superior scaling

properties of the density functional theory (DFT),<sup>17,18</sup> and its innovative use in Car–Parrinello molecular dynamics (CPMD),<sup>19</sup> a great deal of progress has been made in the description of aqueous solutions during the past decade.<sup>20–31</sup> Here we use these methods to calculate the dipole moment of water molecules in the first hydration shell of  $K^+$  and  $Ca^{2+}$  ions, which provide fresh insights and important constraints for polarizable models. In order to give an intuitive understanding of the results in bulk water, we investigate how the dipole moment of the first shell waters evolves as the number water molecules around the ion is increased; it is first suppressed due to the cancelation between the electric fields of the ion and water dipoles in the first shell and then boosted by the polarizing effect of hydrogen bonds as the second shell is filled.

### Methods

The electronic structure calculations on model compounds are performed using DFT with the BLYP functional,<sup>32,33</sup> as implemented in the CPMD package.<sup>34</sup> Although the BLYP functional is known to lead to a slight overstructuring of the first peak in the oxygen–oxygen radial distribution function for bulk water,<sup>25</sup> it performs well for electronic properties such as the dipole moment,<sup>20,25,31</sup> which is the main focus of this work.

The hydration of  $K^+$  and  $Ca^{2+}$  ions in bulk is studied using CPMD simulations for a system consisting of an ion in a periodic box of side  $L = 12.52$  Å with 64 water molecules. A uniform background charge is included to neutralize spurious interactions with neighbor images.<sup>35</sup> The valence-core interaction are described by norm-conserving Trouiller Martins pseudopotentials<sup>36</sup> for K, Ca, and O, and a von Barth–Car analytical pseudopotential<sup>37</sup> for H. The 3s and 3p semicore states of potassium and calcium are treated as valence states. An energy cutoff of 80 Ry is used for the expansion of the valence orbitals

\* To whom correspondence should be addressed.

in a plane-wave basis set. The CPMD simulations are performed at finite temperature (300 K). After classical equilibration, the CPMD simulations are run for 10 ps, of which the first 4 ps is used for equilibration and the next 6 ps is used to collect statistics. This simulation time is found to be sufficient for the convergence of the dipole moment calculations. Agreement of our results with others obtained from longer simulations (see below) provides further justification for the shorter production times used.

Ion–water cluster models are created via geometry optimization for  $M^{q+}(\text{H}_2\text{O})_n$  with  $M^{q+} = \text{K}^+$  or  $\text{Ca}^{2+}$  and  $n = 1, \dots, 6$ . For  $n = 1, \dots, 4$ , the geometries are perfectly symmetric. For  $n = 5$ ,  $\text{K}^+$  and  $\text{Ca}^{2+}$  are inside a squared pyramid ( $C_{4v}$  symmetry). For  $n = 6$ ,  $\text{K}^+$  is inside a trigonal antiprism ( $D_{3h}$  symmetry), and  $\text{Ca}^{2+}$  is in an octahedron ( $O_h$  symmetry). The average ion–oxygen distance is 2.65 Å for  $\text{K}^+$  and 2.35 Å for  $\text{Ca}^{2+}$ , which change little as the water number is increased. To check the stability of these configurations, we have performed CPMD simulations at 300 K, followed by slow annealing, and confirmed that these are indeed the minimum geometries. The choice of  $n = 6$  for the first hydration shell of  $\text{Ca}^{2+}$  is supported by our bulk CPMD simulations using a cut off radius of 3.3 Å in the Ca–O radial distribution function, and the recent CPMD results of Ikeda et al. for the  $\text{Ca}^{2+}$  ion.<sup>38</sup> In the case of  $\text{K}^+$ , the hydration number of the first shell is not very well defined; it could range from 6 to 7 as the cut off radius in the radial distribution function is increased from 3.2 to 3.8 Å. For reasons given in the results section, we prefer to stop at  $n = 6$  in the  $\text{K}^+$  ion cluster calculations.

Maximally localized Wannier functions (MLWF's)<sup>39</sup> are used to monitor intramolecular charge transfers. MLWF's are obtained from a unitary transformation of the occupied molecular orbitals, available from the DFT calculations, to a new set of orbitals which minimize the spread. The MLWF's are appealing because their shapes correspond to chemically intuitive concepts such as covalent O–H bonds and oxygen lone pair orbitals. In addition, the dipole moment of a molecule can be calculated from the position of these new orbitals and their associated charges, together with the position and the charges of the ions, using the classical formula

$$\mu = \sum_{\text{nuclei}} Ze\mathbf{R}_N - \sum_{\text{WFC}} 2e\mathbf{r}_n \quad (1)$$

The positions of the Wannier function centers in a hydrogen-bonded water dimer are indicated in Figure 1a. As seen in the figure, four doubly occupied MLWF centers are located close to each water molecule, two of which are involved in the covalent O–H bonds, and the other two correspond to the lone pair orbitals. Below (a) we show the MLWF's involved in the hydrogen bond for the donor (b) and acceptor (c) water molecules (slightly rotated for a better perspective). The positive and negative phases of the functions are indicated by blue and red, respectively.

Other methods can be used in computation of molecular dipole moments, and they yield slightly different results. For example, using the same CPMD results, the Bader method gives 2.7 D for the dipole moment of water in bulk while the MLWF method gives 3.0 D.<sup>40</sup> Here, we use the MLWF method for easier comparison with the results of similar calculations for the bulk water,<sup>20,25,26</sup> and ion solvation shells.<sup>23,28,30</sup> This method was also able to accurately reproduce the dipole moment of water clusters ( $n = 1, \dots, 5$ ), where experimental data exist.<sup>41</sup>

Electrostatically derived RESP (restrained electrostatic potential) charges are calculated for the model compounds  $M^{q+}(\text{H}_2\text{O})_n$  with  $M^{q+} = \text{K}^+$  or  $\text{Ca}^{2+}$  and  $n = 1, \dots, 6$ , using the Merz–Kollman algorithm<sup>42,43</sup> as implemented in the Gaussian

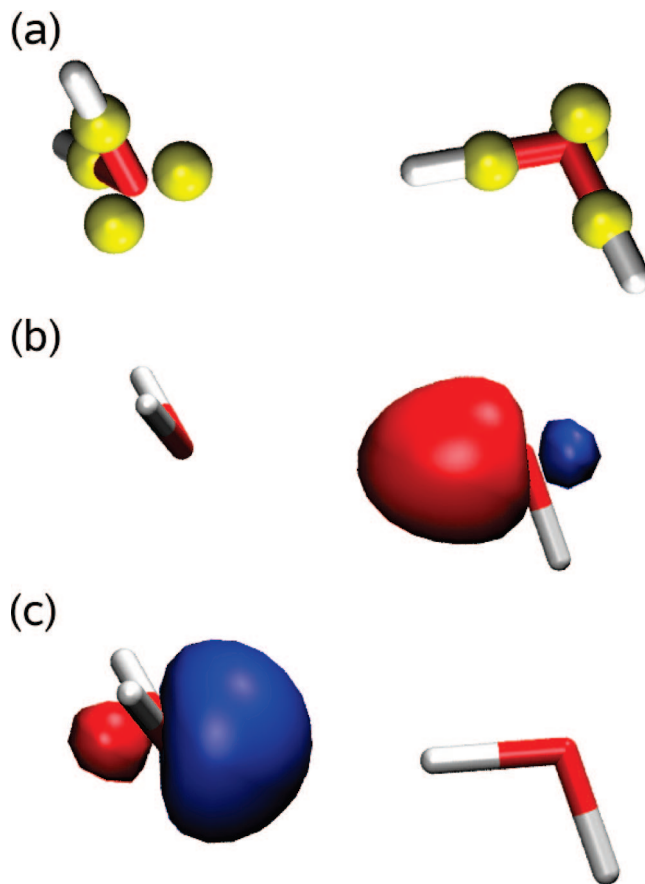


**Figure 1.** (a) Positions of the maximally localized Wannier function (MLWF) centers in a hydrogen-bonded water dimer, indicated by the yellow spheres. Each center corresponds to the center of charge of a 2 electron orbital. Two of the centers correspond to the covalent O–H bonds, and the other two correspond to the lone pair orbitals. The lower figures show the MLWF's involved in the hydrogen bond for the donor (b) and acceptor (c) water molecules (slightly rotated for a better perspective). The positive and negative phases of the functions are indicated by blue and red, respectively.

03 code.<sup>44</sup> The B3LYP functional with the 6-31(d,p) basis sets is used in these calculations. The classical electric field and potential are computed using the fitted charges and probe sites located at the position of the ion and water oxygen. For comparison we have also calculated the classical potential for identical systems using the standard TIP3P charges.

## Results

We first present the results for the dipole moment of water in the first hydration shell of  $\text{K}^+$  and  $\text{Ca}^{2+}$  ions in the bulk phase. To get a better understanding of these results, we deconstruct the system by considering the polarization effects in various ion–water clusters. In particular, we study the how the dipole moment evolves as the first hydration shell is filled in the gas phase and then discuss the polarizing influence of the second shell waters on the first shell waters.

**Polarization of Water in the First Hydration Shell: Bulk Phase.** A system of 64  $\text{H}_2\text{O}$  water molecules with a  $\text{K}^+$  or a  $\text{Ca}^{2+}$  ion is used to model polarization in the condensed phase. We have also repeated the calculations for bulk water to check with earlier results. For bulk water, we obtain a dipole moment of 3.0 D, which is in good agreement with values reported in the literature using similar functionals and the MLWF method in calculation of the dipole moment.<sup>20,25,26,40</sup> For the  $\text{K}^+$  ion

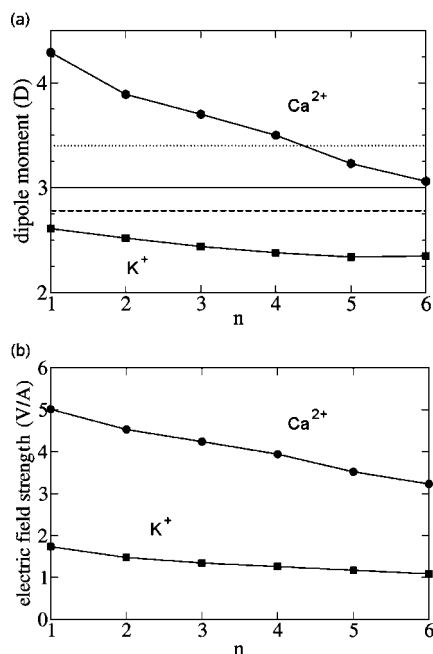


**Figure 2.** (a) Average dipole moment of water molecules in the clusters  $\text{M}^{q+}(\text{H}_2\text{O})_n$  with  $\text{M}^{q+} = \text{K}^+$  or  $\text{Ca}^{2+}$  and  $n = 1, \dots, 6$ . Squares are used for  $\text{K}^+$  and circles for  $\text{Ca}^{2+}$ . The solid line at 3.0 D indicates the average dipole moment of water in bulk, while the dashed and dotted lines indicate the same quantity in the first hydration shell of  $\text{K}^+$  and  $\text{Ca}^{2+}$  ions in bulk water, respectively. (b) The average electric field at the oxygen positions for the clusters in (a).

system, we obtain 2.78 D for the average dipole moment of water in the first hydration shell. This result is obtained using a cut off radius of 3.2 Å, which limits the number of waters in the first shell to 6. Increasing the cut off radius to 3.8 Å and thus allowing 7 waters in the first shell increases the dipole moment by less than 1%, which is within the accuracy of the calculations. Our result is in excellent agreement with two recent calculations of the same quantity,<sup>28,29</sup> whereas another calculation has yielded a slightly higher value (2.93 D).<sup>30</sup> Repeating the same calculation for the  $\text{Ca}^{2+}$  ion system with a cut off radius of 3.3 Å, we find for the dipole moment of the first shell waters 3.4 D. Again this is in good agreement with an earlier calculation<sup>23</sup> but somewhat larger than another one (3.1 D).<sup>30</sup>

The most surprising aspect of these results is that the presence of a  $\text{K}^+$  ion decreases the polarization of waters in the first shell relative to bulk, with the dipole moment dropping from 3.0 to 2.78 D. That is, the electric field of a  $\text{K}^+$  ion is not strong enough to polarize the first shell waters even to the bulk value. Only in the much stronger field of a  $\text{Ca}^{2+}$  ion is this feat achieved. In order to understand this apparently counterintuitive result,<sup>29</sup> it is necessary to deconstruct the ion–water system and consider the contributions of the first and second shell waters to polarization separately.

**Polarization of Water in the First Hydration Shell: Gas Phase.** To see how the dipole moment of a water molecule in the first hydration shell is influenced by the presence of other waters in the shell, we have computed the average water dipole moment for the cluster models  $\text{M}^{q+}(\text{H}_2\text{O})_n$  with  $\text{M}^{q+} = \text{K}^+$  or  $\text{Ca}^{2+}$  and  $n = 1, \dots, 6$ . As shown in Figure 2a, the average dipole moment of water decreases from 2.61 to 2.35 D as the number of waters is increased from  $n = 1$  to 6. (The reason for stopping at  $n = 6$  for the  $\text{K}^+$  cluster is that the seventh water molecule in the periphery makes hydrogen bonds with the other waters, leading to an increase in the average dipole moment against the trend.) Intuitively the reduction in dipole moments follows

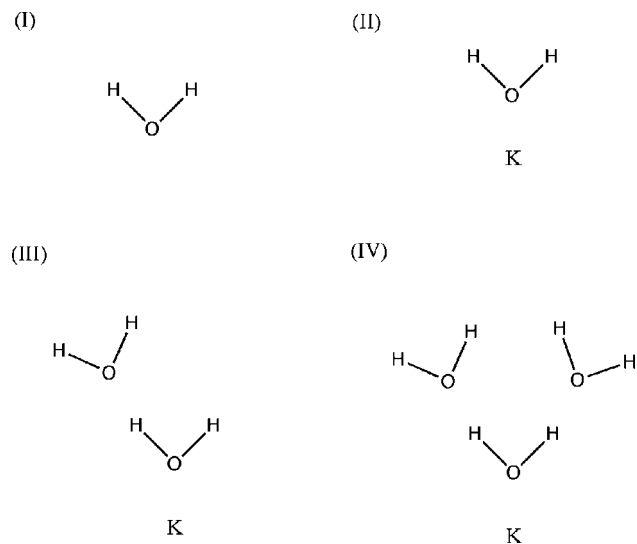


**Figure 3.** Cluster models I–IV used to measure the influence of a  $\text{K}^+$  ion and of the hydrogen bonding environment on the first shell water dipoles.

from the fact that, in all clusters, the water dipoles are in a frustrated configuration with respect to each other, and as a result, contribution of the water dipoles to the electric field at the position of any water molecule is always opposite to that of the ion. Thus as the number of waters is increased, the electric field that polarizes water decreases, which leads to the depicted reduction in its dipole moment.

Because the dipole moment of water is larger in a  $\text{Ca}^{2+}$  cluster compared to a  $\text{K}^+$  cluster, the antipolarizing effect of the first shell waters is even more pronounced in that case. The average dipole moment of water decreases from 4.29 to 3.06 D in going from  $n = 1$  to 6 (Figure 2a). This corresponds to a 50% suppression in the induced dipole moment (i.e., the computed value minus the gas phase value), which is close to the estimate obtained from the classical dipole field formula using a cubic configuration with water dipoles aligned along the ion's field. To quantify these observations, we show in Figure 2b the average electric field at the oxygen positions for the cluster configurations in Figure 2a, which exhibit the same trend as the dipole moments. The dipole moments calculated from the classical formula,  $\mu = \mu_0 + \alpha E$ , using  $\mu_0 = 1.86$  D,  $\alpha = 1.45$  Å<sup>3</sup> for water polarizability, and the electric field values from Figure 2b, are in excellent agreement with those in Figure 2a. An interesting observation here is that, even for a single water molecule ( $n = 1$  in Figure 2a), the field of a  $\text{K}^+$  ion is not strong enough to attain the bulk-like polarization of the water molecule. This underscores the significance of the hydrogen bonded networks and their polarizing effects for bulk water.<sup>27</sup>

**Influence of the Second Hydration Shell.** To demonstrate the polarizing effect of the waters in the second hydration shell, we consider the ion–water clusters shown in Figure 3 (models I–IV). Results of the dipole moment calculations on these models are summarized in Table 1. Inspection of the table indicates that each hydrogen bond acceptor in the second hydration shell polarizes a water in the first shell by about 0.2 D. A similar calculation for 5 water molecules in the tetrahedral ice configuration yields 2.81 D for the dipole moment of the central water, indicating a maximal polarization of 0.24 D per hydrogen bond. In the condensed phase, each water in the first shell can make two hydrogen bonds, which polarizes the dipole of the first shell water by roughly 0.4 D. This result explains why the water dipole moment in the first shell is boosted by

**TABLE 1: Water Dipole Moments in the 1st ( $W_1$ ) and 2nd ( $W_2$ ) Hydration Shells and the Ion–Water Oxygen Distance,  $d$ , for Models I–IV**

	$\mu(W_1)$ (D)	$\mu(W_2)$ (D)	$d(K^+ - W_1)$ (Å)
I	1.85		
II	2.61		2.60
III	2.79	2.51	2.61
IV	3.01	2.52	2.58

about 0.4 D when going from the first shell cluster ( $n = 6$  in Figure 2a) to bulk water in both  $K^+$  and  $Ca^{2+}$  ions (dashed and dotted lines, respectively, in Figure 2a). The slightly larger increase in the water dipole moment for  $K^+$  compared to  $Ca^{2+}$  is presumably due to the first shell waters in  $K^+$  being comparatively more flexible and hence more amenable to hydrogen bonding.

For the  $K^+$  ion, the polarizing effect of the second shell waters completely cancels the antipolarizing effect of the first shell waters and brings the dipole moment closer to the bulk value (dashed line is near the  $n = 1$  result in Figure 2a). However, for the  $Ca^{2+}$  ion, the antipolarizing effect of the first shell waters is about three times stronger than the polarization due to the second shell. This leads to a much larger difference between the dipole moment of water in  $Ca^{2+}(H_2O)$  (the  $n = 1$  result in Figure 2a) and in the first hydration shell of  $Ca^{2+}$  in bulk (the dotted line in Figure 2a). The large variations in the dipole moment of water when the first hydration shell is disrupted means that nonpolarizable force fields with fixed dipoles will run into difficulties in modeling such phenomena. To give an indication of the magnitude of errors involved, we compare below the results of the ab initio calculations with those obtained using the TIP3P model.

**Comparison with Nonpolarizable Models.** The meanfield treatment of water polarization in nonpolarizable force fields may lead to significant errors in the computed energy of a water–ion system when the first hydration shell is disrupted at interfaces, pores, or cavities. To show this, we have derived electrostatically fitted RESP charges for all the  $M^{q+}(H_2O)_n = 1, 6$  models. As the number of water molecules in the clusters is increased from 1 to 6, the optimized charges on the oxygens decrease in parallel to the reduction in the dipole moments. For the  $K^+$  ion this range is  $q = -0.96e$  to  $-0.88e$ , but for the  $Ca^{2+}$  ion, the variation is much larger:  $q = -1.16e$  to  $-0.98e$ . We compute the classical electrostatic potential using both the optimized RESP charges and the standard TIP3P charges ( $q = -0.834e$  for the oxygen). The results are compared in Figure 4 for the  $K^+$  (a) and  $Ca^{2+}$  (b) ions. There is quite a large difference between the computed potentials for the  $Ca^{2+}$  ion so that the dehydration energy will be severely underestimated in the fixed charge model. This example makes it clear that a nonpolarizable force field cannot describe a  $Ca^{2+}$  ion adequately in inhomogeneous systems. Although the situation is not as severe for the  $K^+$  ion, we note that this discrepancy is only for one water oxygen, and the hydration energy could still be substantially underestimated for six water molecules in the first shell.

## Conclusions

We have studied the magnitude of water polarization in the first hydration shell of  $K^+$  and  $Ca^{2+}$  ions using a combination of small cluster model calculations and Car–Parrinello simulations in the condensed phase. We find that the water dipoles in the first hydration shell of an ion counteract the ion's electric field which leads to a reduction in their polarization. This is wholly compensated by the second shell waters in the case of

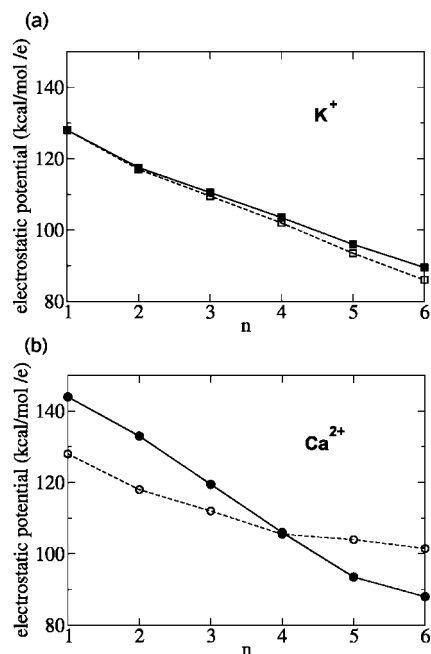


**Figure 4.** Comparison of the electrostatic potentials in the  $M^{q+}(H_2O)_{n=1,6}$  models for (a)  $K^+$  and (b)  $Ca^{2+}$  ions. The electrostatic potential at the position of a water oxygen is computed with the optimized RESP charges (solid lines) and the TIP3P model (dotted lines).

a  $K^+$  ion but only partially compensated for a  $Ca^{2+}$  ion. Combination of these two effects helps to explain why the dipole moment of water in the first hydration shell of a  $K^+$  ion is lower than the bulk value of 3.0 D whereas the opposite is true for a  $Ca^{2+}$  ion. The significant variations observed in the dipole moment of water as the first hydration shell is filled means that the classical force fields with fixed charges will have difficulties in explaining phenomena where the hydration shell of an ion is disrupted. Such situations are very common in biological systems, e.g., ions entering a narrow channel or binding in a cavity.

The mean field description of polarization effects is seen to lead to substantial errors for simple ion–water systems, such as the  $M^{q+}(H_2O)_{n=1,6}$  models, as it is impossible to describe accurately the electrostatic potential for all models with a single charge set. A simple adjustment of the ion's van der Waals parameters may not improve the description of ion coordination to proteins, because other interactions, such as the water–water and water–protein interactions, are also influenced by the polarization effects. Therefore, the current challenge is to design polarizable water models that can provide an accurate description of the hydrogen bonds and polarization effects. We believe that ab initio calculations will play a pivotal role in realizing this goal by providing insights and guidance in development of the polarizable force fields.

**Acknowledgment.** This work was supported by grants from the Australian Research Council and the Swiss National Science Foundation. Calculations were carried out using the SGI Altix clusters at the Supercomputer Facility of the Australian National University and the Australian Center for Advanced Computing and Communications.

**Note Added after ASAP Publication.** This paper was published ASAP on August 12, 2008. Equation 1 was changed. The revised paper was reposted on August 28, 2008.



## References and Notes

- (1) Ball, P. *Chem. Rev.* **2008**, *108*, 74–108.
- (2) Jorgensen, W. L.; Tirado-Rives, J. *Proc. Natl. Acad. Sci.* **2005**, *102*, 6665–6670.
- (3) Ponder, J. W.; Case, D. A. *Adv. Protein Chem.* **2003**, *66*, 27–85.
- (4) Warshel, A.; Parson, W. W. *Q. Rev. Biophys.* **2001**, *34*, 563–679.
- (5) Berendsen, H. J. C.; Postma, J. P. M.; van Gunsteren, W. F.; Hermans, J. In *Intermolecular Forces*; Pullman, B., Ed.; Reidel: Dordrecht, Holland, 1981; pp 331–342.
- (6) Jorgensen, W. L.; Chandrasekhar, J.; Madura, J. D.; Impey, R. W.; Klein, M. L. *J. Chem. Phys.* **1983**, *79*, 926–935.
- (7) Jungwirth, P.; Tobias, D. J. *Chem. Rev.* **2006**, *106*, 1259–1281.
- (8) Chang, T. M.; Dang, X. L. *Chem. Rev.* **2006**, *106*, 1305–1322.
- (9) Berkowitz, M. L.; Bostick, D. L.; Pandit, S. *Chem. Rev.* **2006**, *106*, 1527–1539.
- (10) Allen, T. W.; T; Bastug, T.; Kuyucak, S.; Chung, S. H. *Biophys. J.* **2003**, *84*, 2159–2168.
- (11) Allen, T. W.; Andersen, O. S.; Roux, B. *Biophys. Chem.* **2006**, *124*, 251–267.
- (12) Bucher, D.; Raugei, S.; Guidoni, L.; Dal Peraro, M.; Rothlisberger, U.; Carloni, P.; Klein, M. L. *Biophys. Chem.* **2006**, *124*, 292–301.
- (13) Sham, Y. Y.; Chu, Z. T.; Tao, H.; Warshel, A. *Proteins: Struct. Funct. Genet.* **2000**, *39*, 393–407.
- (14) Guo, H.; Gresh, N.; Roques, B. P.; Salahub, D. R. *J. Phys. Chem. B* **2000**, *104*, 9746–9754.
- (15) Rick, S. W.; Stuart, S. J. *Rev. Comp. Chem.* **2002**, *18*, 89–146.
- (16) Jorgensen, W. L. *J. Chem. Theory Comput.* **2007**, *3*, 1877.
- (17) Hohenberg, P.; Kohn, W. *Phys. Rev.* **1964**, *136*, B 864–871.
- (18) Kohn, W.; Sham, L. J. *Phys. Rev.* **1965**, *140*, A 1133–1138.
- (19) Car, R.; Parrinello, M. *Phys. Rev. Lett.* **1985**, *55*, 2471–2474.
- (20) Silvestrelli, P. L.; Parrinello, M. *Phys. Rev. Lett.* **1999**, *82*, 3308–3311.
- (21) White, J. A.; Schwegler, E.; Galli, G.; Gygi, F. *J. Chem. Phys.* **2000**, *113*, 4668–4673.
- (22) Lyubartsev, A. P.; Laasonen, K.; Laaksonen, A. *J. Chem. Phys.* **2001**, *114*, 3120–3126.
- (23) Bako, I.; Hutter, J.; Palinkas, G. *J. Chem. Phys.* **2002**, *117*, 9838–9843.
- (24) Ohno, K.; Okimura, M.; Akai, N.; Katsumoto, Y. *Phys. Chem. Chem. Phys.* **2005**, *7*, 3005–3014.
- (25) Todorova, T.; Seitsonen, A. P.; Hutter, J.; Kuo, I.-F. W.; Mundy, C. J. *J. Phys. Chem. B* **2006**, *110*, 3685–3691.
- (26) Coudert, F. X.; Vuilleumier, R.; Boutin, A. *ChemPhysChem* **2006**, *7*, 2464–2467.
- (27) Devereux, M.; Popelier, P. J. *Phys. Chem. A* **2007**, *111*, 1536–1544.
- (28) Ikeda, T.; Boero, M.; Terakura, K. *J. Chem. Phys.* **2007**, *126*, 034501.
- (29) Whitfield, T. W.; Varma, S.; Harder, E.; Lamoureux, G.; Rempe, S. B.; Roux, B. *J. Chem. Theory Comput.* **2007**, *3*, 2068–2082.
- (30) Krekeler, C.; Delle Site, L. *J. Phys.: Condens. Matter* **2007**, *19*, 192101.
- (31) Morrone, J. A.; Car, R. Nuclear quantum effects in water, arXiv: 0803.2635 **2008** [cond-mat.soft].
- (32) Becke, A. D. *J. Chem. Phys.* **1993**, *98*, 5648–5652.
- (33) Lee, C.; Yang, W.; Parr, R. G. *Phys. Rev. B* **1988**, *37*, 785–789.
- (34) Hutter, J.; Alavi, A.; Deutsch, T.; Bernasconi, M.; Goedecker, S.; Marz, D.; Tuckerman, M.; Parrinello, M. CPMD. MPI fur Festkorperforschung and IBM Zurich Research Laboratory (1995–1999).
- (35) Makov, G.; Payne, M. C. *Phys. Rev. B* **1995**, *51*, 4014–4022.
- (36) Trouiller, N.; Martins, J. L. *Phys. Rev. B* **1991**, *43*, 1993.
- (37) Sprik, M.; Hutter, J.; Parrinello, M. *J. Chem. Phys.* **1996**, *105*, 1142.
- (38) Ikeda, T.; Boero, M.; Terakura, K. *J. Chem. Phys.* **2007**, *127*, 074503.
- (39) Marzari, N.; Vanderbilt, D. *Phys. Rev. B* **1997**, *56*, 12847–12865.
- (40) Dyer, P. J.; Cummings, P. T. *J. Chem. Phys.* **2006**, *125*, 144519.
- (41) Gregory, J. K.; Clary, D. C.; Liu, K.; Brown, M. G.; Saykally, R. J. *Science* **1997**, *275*, 814–817.
- (42) Singh, U. C.; Kollman, P. A. *J. Comput. Chem.* **1984**, *5*, 129–145.
- (43) Besler, B. H., Jr.; Kollman, P. A. *J. Comput. Chem.* **1990**, *11*, 431–439.
- (44) Frisch, M. J.; *Gaussian 03, revision C.02*; Gaussian, Inc.: Wallingford, CT, 2004.

JP804694U